



Rotavirus-mediated DGAT1 degradation: A pathophysiological mechanism of viral-induced malabsorptive diarrhea

Zheng Liu^{a,b,1}, Hunter Smith^{a,1}, Jeanette M. Criglar^a, Antonio J. Valentin^a, Umesh Karandikar^a, Xi-Lei Zeng^a, Mary K. Estes^{a,c,2} , and Sue E. Crawford^{a,2}

Contributed by Mary K. Estes; received February 15, 2023; accepted October 11, 2023; reviewed by Ulrich Desselberger and Tobias C. Walther

Gastroenteritis is among the leading causes of mortality globally in infants and young children, with rotavirus (RV) causing ~258 million episodes of diarrhea and ~128,000 deaths annually in infants and children. RV-induced mechanisms that result in diarrhea are not completely understood, but malabsorption is a contributing factor. RV alters cellular lipid metabolism by inducing lipid droplet (LD) formation as a platform for replication factories named viroplasm. A link between LD formation and gastroenteritis has not been identified. We found that diacylglycerol O-acyltransferase 1 (DGAT1), the terminal step in triacylglycerol synthesis required for LD biogenesis, is degraded in RV-infected cells by a proteasome-mediated mechanism. RV-infected DGAT1-silenced cells show earlier and increased numbers of LD-associated viroplasm per cell that translate into a fourfold-to-fivefold increase in viral yield ($P < 0.05$). Interestingly, DGAT1 deficiency in children is associated with diarrhea due to altered trafficking of key ion transporters to the apical brush border of enterocytes. Confocal microscopy and immunoblot analyses of RV-infected cells and DGAT1^{-/-} human intestinal enteroids (HIEs) show a decrease in expression of nutrient transporters, ion transporters, tight junctional proteins, and cytoskeletal proteins. Increased phospho-eIF2 α (eukaryotic initiation factor 2 alpha) in DGAT1^{-/-} HIEs, and RV-infected cells, indicates a mechanism for malabsorptive diarrhea, namely inhibition of translation of cellular proteins critical for nutrient digestion and intestinal absorption. Our study elucidates a pathophysiological mechanism of RV-induced DGAT1 deficiency by protein degradation that mediates malabsorptive diarrhea, as well as a role for lipid metabolism, in the pathogenesis of gastroenteritis.

rotavirus | DGAT1 | lipid droplet | viroplasm | proteasome degradation

Lipid droplets (LDs), previously considered simple storage structures for neutral lipids, are now recognized as dynamic intracellular organelles involved in diverse biological processes such as membrane trafficking, signal transduction, and modulation of immune and inflammatory responses (1). LDs consist of a hydrophobic core of the neutral lipid triacylglycerol (TAG) and cholesterol esters that are surrounded by a phospholipid monolayer (2). The phospholipid monolayer contains surface proteins that regulate lipid metabolism. Despite the increased number of LD studies in recent years, the mechanism(s) of LD biogenesis remain poorly understood. The classic model of LD biogenesis posits that LDs arise from the endoplasmic reticulum (ER) in a mechanism that resembles budding (3). A complex composed of LD assembly factor 1 protein and the ER-resident protein seipin determines the site of LD formation in the ER membrane and facilitates LD biogenesis (4). The mechanism of LD biogenesis requires the 1) de novo synthesis and remodeling of ER membrane phospholipids and 2) integration of LD-associated proteins (5).

TAGs in the LD are produced by an elaborate biosynthetic pathway (3). The terminal step of TAG synthesis is the conversion of diacylglycerol (DAG) and acyl-CoA into TAG catalyzed by ER-localized DAG acyltransferases DGAT1 (Diacylglycerol O-acyltransferase 1) and DGAT2. Although catalyzing the same reaction, DGAT1 and DGAT2 are substantially different. Neither share sequence homology, redundant functions, or cellular expression patterns (6), suggesting distinct roles for each in TAG metabolism. In cultured cell lines, confocal microscopy showed that DGAT1 is only detected in the ER, whereas DGAT2 colocalizes with the ER, LDs, and mitochondria (7). In mice, both DGAT1 and DGAT2 are expressed in the intestine, while in humans, only DGAT1 is expressed in the intestine (8).

Patients with biallelic mutations in DGAT1 manifest with severe chronic diarrhea and/or vomiting, hypoalbuminemia, and/or (fatal) protein-losing enteropathy with intestinal failure (8–10). Duodenal biopsies from patients with DGAT1 deficiency show either loss or mislocalization of the apical membrane transporters NHE3, SGLT1, the dipeptidyl peptidase IV (DDP4), and the junctional proteins occludin and claudin 4 in enterocytes (10). Similar protein localization defects, as well as increased cellular lipid levels, are observed in Caco2-BBe DGAT1 knockdown cells (10). These studies suggest that loss of DGAT1 expression elicits global changes in enterocyte apical brush border protein polarized

Significance

Lipid droplets (LDs) play emerging roles in diabetes, obesity, and heart disease. Although LDs are implicated in the replication of several enteric viral pathogens, like rotavirus (RV) that causes severe diarrhea, a role for LDs in gastrointestinal pathogenesis has not been identified. RV induces and requires LDs to assemble virus replication factories. We demonstrate RV infection leads to the degradation of diacylglycerol O-acyltransferase 1 (DGAT1), the enzyme responsible for the terminal step in triacylglycerol synthesis needed for LD formation. Loss of DGAT1 decreases expression of key nutrient and ion transporters and junctional proteins required for normal enterocyte homeostatic function. Our study elucidates a pathophysiological mechanism of RV-induced malabsorptive diarrhea and a role for lipid metabolism in the pathogenesis of gastroenteritis.

Author contributions: Z.L., H.S., J.M.C., A.J.V., U.K., X.-L.Z., M.K.E., and S.E.C. designed research; Z.L., H.S., J.M.C., A.J.V., U.K., X.-L.Z., and S.E.C. performed research; Z.L. and X.-L.Z. contributed new reagents/analytic tools; Z.L., H.S., J.M.C., A.J.V., U.K., M.K.E., and S.E.C. analyzed data; and Z.L., H.S., J.M.C., M.K.E., and S.E.C. wrote the paper.

Reviewers: U.D., University of Cambridge; and T.C.W., Harvard School of Public Health.

The authors declare no competing interest.

Copyright © 2023 the Author(s). Published by PNAS. This article is distributed under [Creative Commons Attribution-NonCommercial-NoDerivatives License 4.0 \(CC BY-NC-ND\)](https://creativecommons.org/licenses/by-nc-nd/4.0/).

¹Z.L. and H.S. contributed equally to this work.

²To whom correspondence may be addressed. Email: mestes@bcm.edu or crawford@bcm.edu.

This article contains supporting information online at <https://www.pnas.org/lookup/suppl/doi:10.1073/pnas.2302161120/-/DCSupplemental>.

Published December 11, 2023.

trafficking and lipid metabolism, which may account for enterocyte malabsorption and subsequent diarrhea.

Many intracellular pathogens, including viruses, bacteria, and parasites, target and require host LDs for replication (11). RV (rotavirus), a leading cause of severe dehydrating gastroenteritis in infants and children under the age of 5, requires LDs to form viroplasm (12, 13). Viroplasms are composed of both viral and cellular proteins that form in association with components of LDs, within which viral replication and immature particle assembly occur. The interaction of two RV nonstructural proteins, NSP2 and NSP5, is required for viroplasm formation (14, 15). Formation of LDs appears to be vital for RV replication as compounds that block LD formation or disperse LDs significantly decrease the number and size of viroplasms and the production of infectious progeny (13, 16). In addition, the LD-associated proteins PLIN1 and PLIN2 and the lipophilic stain Nile red colocalize with NSP2 and NSP5 in viroplasms (13). These results indicate that viroplasms either form with or on LDs (17). However, the mechanisms of LD biogenesis that are exploited by RV for viroplasm formation remain to be deciphered.

The epithelial cells of the gastrointestinal tract play key roles in the digestion, absorption, and metabolism of nutrients. RV is transmitted via the fecal-oral route and infects enterocytes, tuft, and enteroendocrine cells in the intestinal tract (12, 18). RV induces diarrhea through a combination of mechanisms including intestinal secretion (stimulated by the RV-encoded enterotoxin NSP4), activation of the enteric nervous system, and destruction of the absorptive enterocytes, which leads to malabsorption (12). A role for RV-altered lipid metabolism in RV-induced diarrhea has not been identified.

Although a link between RV-mediated epithelial dysfunction and the level of DGAT1 expression has not been previously identified, RV-infected cells show deficits of apically localized proteins similar to those seen in human biopsies of DGAT1-deficient children with diarrhea and in Caco2-BBe DGAT1 knockdown cells (10, 19). Studies in RV-infected mouse pups demonstrated a reduction of sodium-dependent glucose cotransporter 1 (SGLT1) expression from the brush border of enterocytes along the villi at 1 d postinfection (20). RV infection of polarized Caco-2 cells resulted in disorganization of apical brush border enzymes and junctional proteins occludin (21), claudin 1, and ZO-1 (22) reminiscent of DGAT1-deficient duodenal patient biopsies and indicative of loss of barrier integrity. Thus, RV infection-induced reduction or mislocalization of these proteins may lead to epithelial dysfunction that results in diarrhea.

The present study was designed to examine whether RV exploitation of LD biogenesis and regulation of DGAT1 enhances virus replication and pathogenesis. We used the well-established monkey kidney cell (MA104) model of RV infection as well as stem cell-derived human intestinal enteroids (HIEs) for these studies. HIEs have revolutionized the study of enteric viruses like RV (23, 24). These multicellular, nontransformed cultures retain host genetic properties, cellular organization and polarity, as well as recapitulate the physiology of the human gastrointestinal epithelium. Thus, they serve as biologically and physiologically relevant model systems for studying human enteric infections.

Results

RV Viroplasms Colocalize with PLIN1 LDs. LD formation is a critical step in viroplasm formation and the subsequent production of infectious virus (13). RV viroplasms were previously reported to colocalize with components of LDs (13). We used confocal microscopy to visualize viroplasm-dependent nonstructural proteins NSP2 and NSP5 and the LD-associated protein PLIN1. A previous report

used Nile Red to detect LDs; however, Nile Red nonspecifically labels all lipid-containing organelles and intracellular membranes. Therefore, we used LipidTOX™, a neutral lipid-specific stain that has an extremely high affinity for neutral lipid, such as that in LD cores, to detect LDs. We observed that viroplasms colocalized with PLIN1 LDs (*SI Appendix, Fig. S1, Top*) and neutral lipid (*SI Appendix, Fig. S1, Bottom*) as previously reported (13, 17, 25). These results confirm that components of LDs colocalize with viroplasms in RV-infected cells.

DGAT1 Interacts with dNSP2 but Not vNSP2. To gain a better understanding of viroplasm/LD interactions, we first sought to identify cellular proteins that interact with NSP2 and might be involved in viroplasm/LD formation. We previously identified two distinct forms of NSP2 that differ in temporal appearance, localization, and conformation in the RV-infected cell (26). These two forms of NSP2: dispersed NSP2 (dNSP2) and viroplasm-associated NSP2 (vNSP2) were detected with specific monoclonal antibodies (26). Mass spectroscopy of proteins that coimmunoprecipitated (IP-MS) with dNSP2, vNSP2, or both identified DAG modifying enzymes. Since DGAT1 conversion of DAG and acyl-CoA into TAG is the rate-limiting step in the TAG synthesis pathway, we evaluated whether DGAT1 interacts with either dNSP2 or vNSP2. Immunoprecipitation (IP) of DGAT1 and western blot analyses using the dNSP2 or vNSP2 monoclonal antibodies showed that DGAT1 coprecipitates with only dNSP2 and not vNSP2 (Fig. 1A).

We next determined whether the interaction of dNSP2 with DGAT1 is specific by investigating whether DGAT1 is in a complex with other ER-localized proteins that were detected in our NSP2 IP-MS. IP of acyl-coenzyme A:monoacylglycerol acyltransferase 3 (MGAT3) that catalyzes the synthesis of DAG from monoacylglycerol (MAG) and inositol 1,4,5-trisphosphate receptor (IP3R) one of the three isoforms of the IP3R ion channel that releases calcium from the ER, and western blot analyses using the dNSP2 monoclonal antibody showed that both MGAT3 and IP3R3 coprecipitate dNSP2 (Fig. 1B, *Left* panels). We next determined whether DGAT1 forms a complex with either MGAT3 or IP3R3 in mock or RV-infected cells (Fig. 1B, *Right* panels). Western blot analyses showed that DGAT1 does not interact with MGAT3 or IP3R3 in either mock or RV-infected cells indicating that dNSP2 can target specific ER-membrane proteins that are not associated in a protein complex (Fig. 1B, *Right* panels).

Viroplasm Formation Is Accelerated in DGAT1-Silenced Cells. We next sought to determine whether dNSP2 interaction with DGAT1 plays a role in viroplasm/LD formation. Therefore, we silenced DGAT1 in RV-infected cells and used confocal microscopy to evaluate the kinetics of viroplasm/LD formation. We found that viroplasm/LD formation occurs earlier in the DGAT1-silenced cells compared to irrelevant siRNA-transfected cells (Fig. 1C), with a significant increase in the percent of cells containing viroplasms (Fig. 1D) as well as the number of viroplasm/LDs per cell (Fig. 1E). This result indicated that our original hypothesis that dNSP2 interaction with DGAT1 might induce viroplasm/LD formation was incorrect. Earlier and increased formation of viroplasms/LDs in DGAT1-silenced cells, suggested that the absence of DGAT1 may regulate LD budding into the cytoplasm.

RV Yield Increases in DGAT1-Silenced or Knockout Cells. To determine the effect of DGAT1 on RV replication, we measured virus yields from RV-infected, DGAT1-silenced, and irrelevant siRNA-transfected MA104 cells. The yield of virus increased fourfold in RV-infected, DGAT1-silenced cells compared to

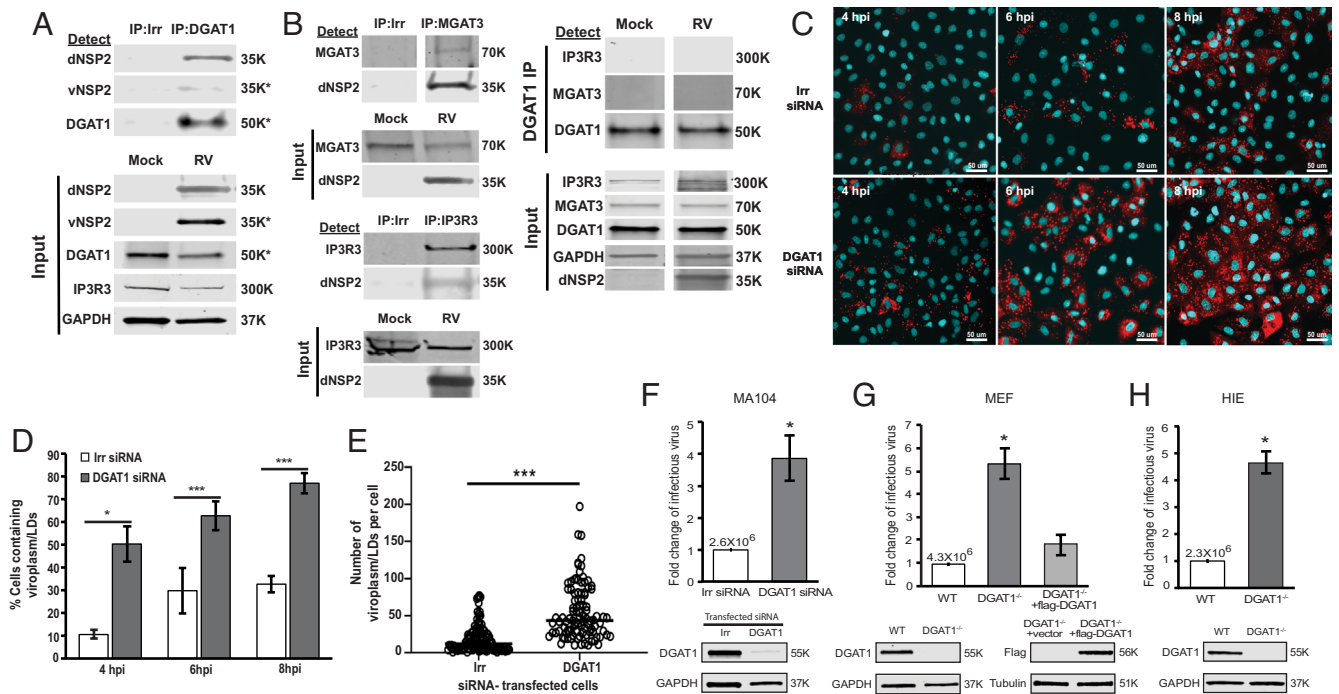


Fig. 1. Silencing DGAT1, which interacts with dNSP2, increases the numbers of viroplasm formed and RV yield. (A) IPs were performed with RV-infected cell lysates harvested at 4 hpi using irrelevant (Irr, mCherry) or DGAT1 antibody. Western blots of the precipitated samples were probed with mouse anti-dNSP2, mouse anti-vNSP2, or rabbit anti-DGAT1. Input proteins in mock-infected or RV-infected total cell lysates used for the IPs were detected using the antibodies indicated to the left of the blots. IP3R3 and GAPDH were detected as loading controls for the input lysates. SDS-PAGE was run in reducing conditions: IP dNSP2, IP3R3, GAPDH, or nonreducing conditions: vNSP2, DGAT1. (B, Left panels) IPs were performed with RV-infected cell lysates using Irr, MGAT3, or IP3R3 antibody. Western blots of the precipitated samples were probed with mouse anti-dNSP2 or the IP antibody. Input proteins in mock-infected or RV-infected total cell lysates that were used for the IPs were detected using the antibodies indicated to the left of the blots. (B, Right panels) IPs were performed with mock or RV-infected cell lysates using DGAT1 antibody. Western blots of the precipitated samples were probed with IP3R3, MGAT3, and DGAT1 IP antibody. Input proteins in mock-infected or RV-infected total cell lysate that was used for the IPs were detected using the antibodies indicated to the left of the blots. (A and B) The primary antibodies were detected with secondary antibodies conjugated to IRDye680RD and IRDye800CW. Infrared images of immunoblots were acquired using the Odyssey CLx and analyzed using Image Studio Lite software. Molecular weights are indicated to the right of each blot. (C) MA104 cells transfected with an irrelevant siRNA (Upper) or DGAT1 siRNA (Lower) were SA11 RV-infected (MOI 3) and then fixed and permeabilized at the indicated times postinfection. Viroplasms were detected using antibody against vNSP2 (red) and nuclei were stained with DAPI (blue). The experiment was performed twice. (Scale bar, 50 μ m.) (D) Quantification of the number of cells containing viroplasms in C. At least 800 cells from 3 to 6 random fields were counted at each time point and condition. Data represent the mean, and error bars represent the SD. (E) Quantification of the number of viroplasm/LDs per cell at 4 hpi. The bar represents the mean. * $P < 0.05$ and *** $P < 0.005$, Student *t* test. (F–H) Effect of silencing or knocking out DGAT1 in RV-infected cell lines and HIEs. Cells were infected with RV (MOI 1). Cells and media were harvested at 24 hpi, and the progeny virus was quantified by fluorescent focus assay. The virus titer from irrelevant (Irr) siRNA transfected or WT cells is shown above the white bar. Each assay was performed twice with three replicates. Error bars represent the SD. * $P < 0.05$, Student *t* test. Western blot detection of DGAT1 to confirm DGAT1 silencing or knock out and GAPDH loading control in each respective cell type is shown below each graph. Molecular weights are indicated to the right of each blot. (F) MA104 cells transfected with Irr or DGAT1 siRNA. (G) Wild-type DGAT1^{+/+} (WT), DGAT1 deficient (DGAT1^{-/-}), or DGAT1^{-/-} MEFs transfected with flag-tagged DGAT1. (H) WT or DGAT1^{-/-} HIEs.

irrelevant siRNA-transfected cells (Fig. 1F). This result contrasts with a previous report that silencing DGAT1 resulted in a 1.4-fold decrease in RV yield (27). To confirm our findings with complete loss of DGAT1, we determined the yield of virus from infected wild-type DGAT1^{+/+} (WT) and DGAT1^{-/-} mouse embryo fibroblasts (MEFs). Similar to DGAT1-silenced MA104 cells, the yield of virus in DGAT1^{-/-} MEFs was ~fivefold higher than in WT MEFs (Fig. 1G). Critically, expression of flag-tagged DGAT1 in DGAT1^{-/-} MEFs reduced the yield of virus similar to levels detected in WT MEFs (Fig. 1G). These results show that silencing DGAT1 increases RV yield.

We next determined whether knocking out DGAT1 in HIEs also resulted in an increase in RV replication. We previously demonstrated that HIEs, a new, biologically relevant human model system, can be used to study human RV pathophysiology (23, 24). Sequencing the genome of the DGAT1^{-/-} HIE line generated from a single cell clone confirmed that DGAT1 was knocked out; a 213-bp fragment was deleted in DGAT1 (SI Appendix, Fig. S2A), and western blot analysis showed a complete loss of DGAT1 expression in DGAT1^{-/-} cells (SI Appendix, Fig. S2B). We also observed that the growth of the DGAT1^{-/-} cells was impaired

compared to the WT HIE line (SI Appendix, Fig. S3). HIE infections with a human RV, Ito, resulted in a fourfold-to-fivefold increase in infectious RV in DGAT1^{-/-} HIEs compared to WT HIEs. This verifies that knockout of DGAT1 in HIEs enhances RV yield (Fig. 1H).

Viroplasm-Associated Neutral Lipid Accumulates in Cells Prior to Infection.

DGAT1 catalyzes the terminal and committed step in triglyceride synthesis. Therefore, we next examined whether the neutral lipids detected in viroplasm/LDs were synthesized before or during RV infection. To track the neutral lipids destined for incorporation into viroplasms, we performed a pulse-chase experiment using fluorescently labeled dodecanoic acid, BODIPYTM 558/568 C12, a fatty acid analogue that incorporates into neutral lipid molecules. In uninfected MA104 cells metabolically labeled prior to RV infection and imaged at 3 hpi, BODIPYTM 558/568 C12 was distributed within the ER, and manifested as red reticular structures (SI Appendix, Fig. S4A, cells without asterisks), while in the RV-infected cells, all viroplasms colocalized with BODIPYTM 558/568 C12 (SI Appendix, Fig. S4A, cells with asterisks). In contrast, in cells

labeled at 2 to 3 h postinfection and imaged at 3 hpi, most of the BODIPY 558/568 C12-labeled LDs did not colocalize with NSP5 in viroplasms (SI Appendix, Fig. S4B). These results suggest that the TAGs in the viroplasm/LDs were synthesized and accumulate in the cell prior to infection and that during RV-infection, the cells continue to uptake fat and make new LDs that do not colocalize with viroplasm/LDs. This result is consistent with a previous report showing RV replication is inhibited to a greater extent by blocking fatty acid synthesis prior to infection rather than during or after infection (28).

DGAT1 Is Degraded in RV-Infected Cells by a Proteasome-Dependent Mechanism. Our findings that RV infection of DGAT1-silenced cells increased virus yield, while overexpression of DGAT1 in the DGAT1^{-/-} MEF cells reduced virus yield, raised the possibility that the levels of DGAT1 are virus regulated during RV infection. Therefore, we evaluated DGAT1 protein expression in RV-infected MA104 cells using western blot. We found that endogenous DGAT1 levels decrease as the RV nonstructural protein NSP2 increases during RV infection (Fig. 2A and B). To determine whether DGAT1 loss was proteasome-dependent, the cell-permeable proteasome inhibitor MG132 was added to the cultures following RV infection. The addition of MG132 prevented the degradation of DGAT1 in MA104 cells (Fig. 2C) indicating that DGAT1 is degraded by a proteasome-dependent mechanism in RV-infected MA104 cells.

To determine whether RV-infection of HIEs results in DGAT1 degradation, we performed western blot analysis for DGAT1 in

RV-infected HIEs. We found that RV-infection decreased the level of DGAT1 in HIEs and that the addition of MG132 prevented DGAT1 degradation (Fig. 2D), recapitulating our results in monkey kidney cells.

DGAT1 Interacts with Ubiquitinated dNSP2. Proteins destined for degradation in the proteasome are tagged with ubiquitin (29). To determine the mechanism of DGAT1 proteasomal degradation, we assessed whether DGAT1 and/or NSP2 were ubiquitinated and might mediate proteasomal degradation. MA104 cells were transfected with a plasmid expressing human influenza hemagglutinin (HA)-tagged ubiquitin, and then mock- or RV-infected. HA was immunoprecipitated to pull down HA-ubiquitinated proteins and western blots of the precipitates were probed to detect DGAT1 or dNSP2. DGAT1 was immunoprecipitated in both the mock- and RV-infected cells (Fig. 2E). Detection of HA-ubiquitinated DGAT1 in the mock-infected cells suggests that this likely represents endogenous DGAT1 undergoing normal turnover (Fig. 2E). We also detected dNSP2 from the precipitates of the RV-infected cells (Fig. 2E). From these results, we show that one or both proteins are ubiquitinated during RV infection.

K48-linked polyubiquitination is a specific ubiquitination that functions to mark target proteins for proteasomal degradation (29). We examined whether the dNSP2 that interacts with DGAT1 is K48 polyubiquitinated to further test whether the ubiquitinated dNSP2-DGAT1 complex could be critical to DGAT1 degradation. DGAT1 was immunoprecipitated from mock- or RV-infected MA104 cell lysates (Input, Fig. 2F).

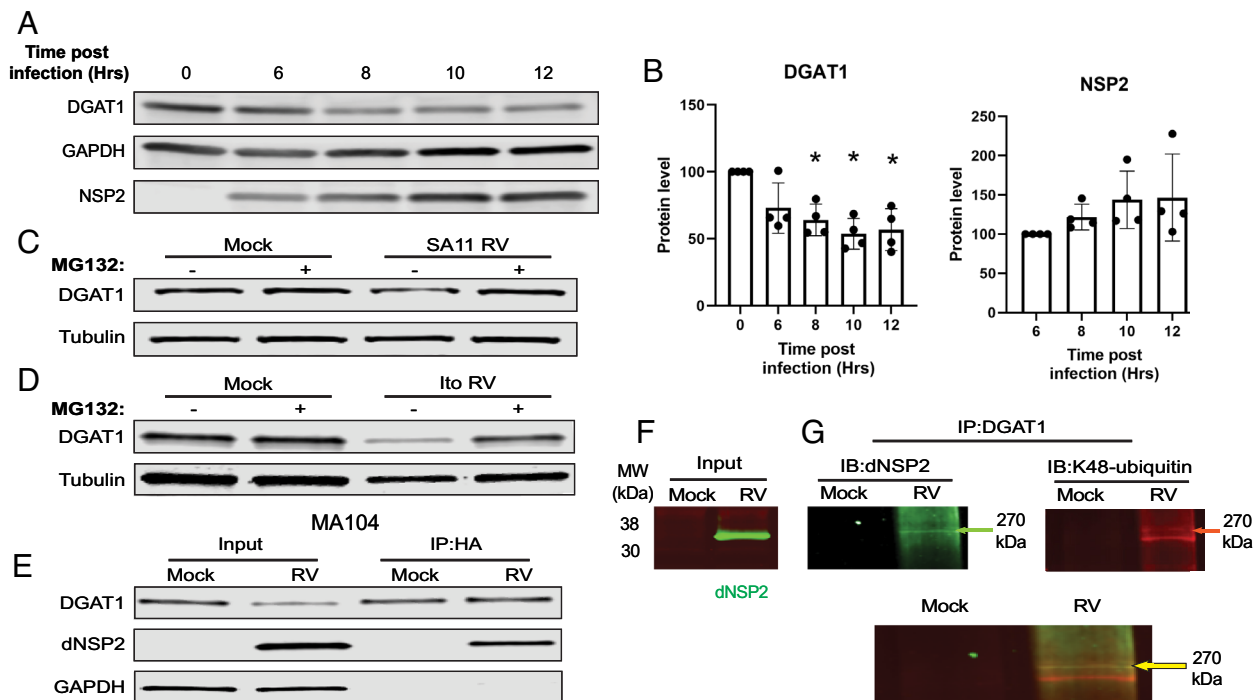


Fig. 2. DGAT1 is degraded in RV-infected cells by a proteasome-dependent mechanism. (A) MA104 cells were mock- or RV-infected by SA11 4F over 12 h. Cells were harvested at specific time points. (B) Protein levels of DGAT1 and NSP2 were quantified, and normalized to GAPDH, at the indicated time points using the ImageStudio analysis function. (C) MA104 cells or (D) HIEs were mock- or RV-infected by (C) SA11 4F or (D) the human RV strain Ito in the absence (-) or presence (+) of the proteasome inhibitor MG132. Cells were harvested at 4 hpi for MA104 cells or 24 hpi for HIEs and cell lysates were analyzed by western blot to detect DGAT1 or GAPDH as a loading control. (E) MA104 cells were transfected with a HA-tagged ubiquitin-expressing plasmid. Cells were mock- or SA11 4F-infected at a MOI of 10. Cells were harvested at 4 hpi, and IPs were performed using antibody against HA. The lysates and precipitated samples were analyzed by SDS-PAGE, and western blots were probed with antibodies to detect DGAT1, dNSP2, and GAPDH as a loading control for the input. (F) IP input: Mock- and RV-infected MA104 cell lysates were probed with antibody against dNSP2 (green). (G and H) IP was performed on mock- and RV-infected lysates in (F) using antibody against DGAT1. The precipitated samples were analyzed by SDS-PAGE, and the same western blot was probed with antibodies to detect dNSP2 (green) and K48-ubiquitin (red) (IB = immunoblot). (H) Merge of the western blots shown in (F). The primary antibodies were detected with secondary antibodies conjugated to IRDye680RD or IRDye800CW. Infrared images of immunoblots were acquired using the Odyssey CLx and analyzed using Image Studio Lite software.

A western blot of the precipitates was probed to detect dNSP2 and K48 ubiquitin (Fig. 2*G*) using the LiCor dual-fluorescence system; both antibodies detected a high molecular weight band, ~270 kDa, which suggests that dNSP2 is polyubiquitinated (Fig. 2*H*). These results indicate that DGAT1 interacts with polyubiquitinated dNSP2; however, future experiments are needed to confirm that DGAT1 is degraded by interacting with ubiquitinated dNSP2.

DGAT2 Is Expressed in Undifferentiated, but Not Differentiated HIEs, and Is Not Up-Regulated Following RV Infection. DGAT2, an isoenzyme of DGAT1, has been proposed to compensate for DGAT1 in LD formation in human DGAT1-deficient HIEs (30). To determine whether RV-mediated DGAT1 degradation in HIEs up-regulates *Dgat2* for TAG synthesis and LD formation, we used RNA-seq to ascertain the levels of *Dgat1* and *Dgat2* mRNA in mock- or human RV-infected HIE cultures established from two different individuals from each segment of the small and large intestine. *Dgat1* was highly expressed in all segments of the small intestine, as well as the colon [SI Appendix, Fig. S5*A*, average ~12,000 Fragments Per Kilobase of transcript per Million mapped reads (FPKM) in all segments]. In contrast, *Dgat2* expression was less than *Dgat1* (SI Appendix, Fig. S5*B*, average ~500 FPKM). RV infection did not increase the expression of either *Dgat1* or *Dgat2* (SI Appendix, Fig. S5*A* and *B*). In the current study, differentiated HIEs were used for all experiments because RV only infects differentiated HIEs (23). Western blot analysis to assess protein expression levels found DGAT2 was only expressed in undifferentiated HIEs (SI Appendix, Fig. S5*C*, *Left*). Additionally, DGAT2 expression was not up-regulated in RV-infected differentiated HIEs (SI Appendix, Fig. S5*C*, *Right*). These results indicate that DGAT2 protein expression is down-regulated in differentiated HIEs and DGAT2 does not compensate for DGAT1 in RV-infected cells where DGAT1 is degraded for LD formation.

RV-Mediated DGAT1 Degradation Mimics the Phenotype of DGAT1 Deficiency Disease. DGAT1 deficiency is included in a group of rare inherited congenital intestinal diarrheal disorders that are characterized by intractable, sometimes life-threatening, diarrhea and nutrient malabsorption. Biopsies from children with DGAT1 deficiency show global changes in enterocyte polarized protein trafficking that could account for the deficits in absorption and the subsequent diarrhea observed in these children (10). Therefore, we next determined whether RV-mediated DGAT1 degradation in HIEs results in phenotypic changes similar to those observed in biopsies from DGAT1-deficient children. Although few histopathological studies of samples from patients with RV infection have been carried out, villus blunting was observed (31). Since HIEs do not have typical villus structures, villus blunting could not be assessed in HIEs. However, epithelial thinning was observed in RV-infected HIEs (Fig. 3*A*, quantification of cell height shown in Fig. 3*B*). In addition, similar to DGAT1^{-/-} cells, a previous lipidome analysis established that RV infection results in increased levels of DAG and phospholipids in HIEs (10, 32).

To determine whether RV-mediated DGAT1 degradation results in trafficking defects similar to those observed in DGAT1 deficiency biopsies, the localization of apical brush border proteins [sucrase-isomaltase (SI), sodium-hydrogen exchanger (NHE3), and ezrin], the cell adhesion molecule E-cadherin, and the junctional complex proteins JAM-1 (junctional adhesion molecule 1) and occludin, were assessed in the DGAT1^{-/-} HIEs. Similar to findings in studies of small intestine biopsies from RV-infected or

DGAT1-deficient patients utilizing immunofluorescence, we observed mislocalized, reduced expression, or complete loss of NHE3 and ezrin on RV-infected 3D HIEs, and E-cadherin, occludin, JAM-1, and SI from RV-infected HIEs on transwells (Fig. 3*C* and *D*) (10, 19). Loss of apical SI and NHE3 was observed in our 3D DGAT1^{-/-} HIEs (Fig. 3*E*) similar to the previously published report (10).

RV-Mediated DGAT1 Degradation and DGAT1 Deficiency Result in Loss or Reduction of Apical Brush Border Enzymes.

It has been hypothesized that the altered polarized trafficking of apical brush border and tight junctional proteins accounts for the deficits in absorption and the subsequent diarrhea observed in DGAT1-deficient children (10). However, the level of the expressed proteins was not assessed. Therefore, we determined the level of protein expression in mock and RV-infected HIEs, and WT and DGAT1^{-/-} HIEs using western blot analysis. A substantial reduction in the expression level of SI, NHE3, villin, ezrin, and E-cadherin, but not claudin 4, was observed in RV-infected and DGAT1^{-/-} HIEs, compared to mock and parental HIEs, respectively (Fig. 4*A*). These western blots, together with the confocal microscopy results, reveal that RV-mediated DGAT1 degradation or DGAT1 knockout leads to the specific loss or lack of expression of these proteins rather than a global alteration in trafficking. RV-induced malabsorptive diarrhea was thought to be attributed to a loss of enterocytes. These results indicate dNSP2-mediated DGAT1 degradation leads to decreased expression of proteins required for normal enterocyte function.

To determine the mechanism for decreased cellular protein expression, we assessed whether the eukaryotic translation initiation factor 2 alpha (eIF2 α), the regulator of global cellular translation, is phosphorylated. Phosphorylated eIF2 α (P-eIF2 α) inhibits global cellular translation (33). Compared to WT HIEs, P-eIF2 α is increased in DGAT1^{-/-} HIEs (Fig. 4*B*). RV infection also induces the phosphorylation of eIF2 α and the inhibition of cellular protein synthesis (34, 35). Increased P-eIF2 α in DGAT1^{-/-} HIEs (observed in Fig. 4*B*) and RV-infected cells may be a mechanism for the downregulation of protein expression that leads to the pathophysiology of malabsorptive diarrhea.

Discussion

LDs are increasingly recognized as dynamic organelles that not only store lipid but are an essential platform for various cellular processes, including lipid metabolism, cell signaling, protein storage, autophagy, immunity, and the replication of pathogenic viruses (36). Numerous intracellular pathogens (bacterial, parasitic, and viral) exploit LDs as an energy source, a replication site, and/or a mechanism of immune response evasion (37). RV induces and requires LDs as a component of the viroplasm, a cytoplasmic virus replication factory (13, 25). As many fundamental features of LD biology remain obscure, such as the molecular mechanisms that signal LD budding from the ER, we used RV as a tool to define how LDs are induced upon infection. We found in RV-infected cells and HIEs that the dispersed form of RV NSP2 (dNSP2) interacts with DGAT1, dNSP2 is K48 polyubiquitinated, and DGAT1 is degraded by the proteasome. We propose that RV mediates DGAT1 degradation through interaction with K48 polyubiquitinated dNSP2, which provides a new function for this nonstructural protein. Furthermore, silencing DGAT1 leads to earlier formation and increased numbers of viroplasm/LDs as well as increased viral yields. Together, these results indicate that DGAT1 degradation may be a trigger for LD formation that enhances virus replication. We also found that RV-mediated

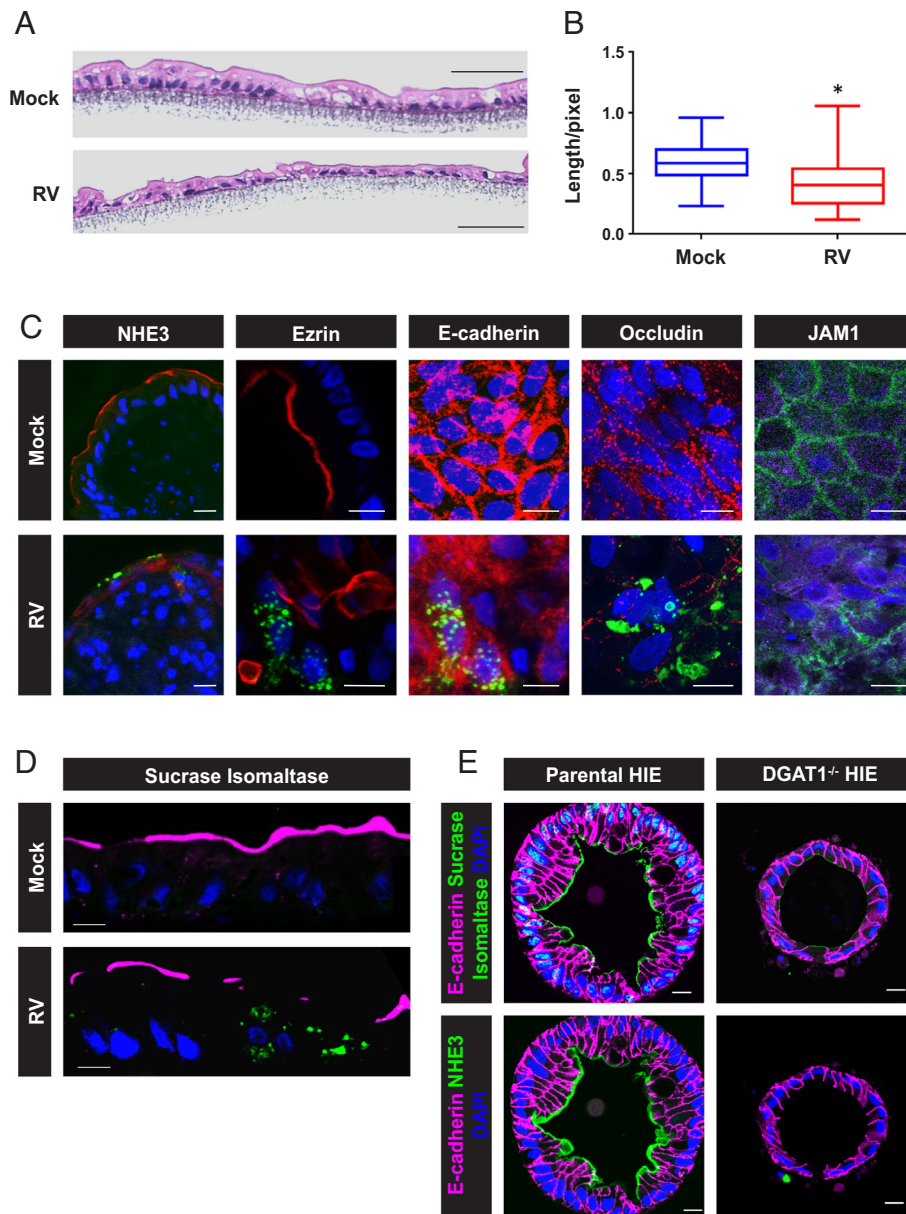


Fig. 3. Epithelial thinning is observed in RV-infected HIEs and RV infection and DGAT^{-/-} results in loss of apical brush border protein localization. (A) Representative hematoxylin and eosin-stained paraffin sections of mock- and RV-infected HIE monolayers on a transwell. (B) Epithelial thickness was measured from 5 different sections, ~60 measurements, for mock- or RV-infected HIE sections. $P < 0.0001$, Student t test. (C) Mock- and RV-infected paraffin sections of whole mount 3D HIEs, or HIEs on a transwell were probed with antibodies to detect the indicated cellular protein (red; Exception: JAM-1 is in green) or NSP2 (green). (Scale bar, 25 μm .) SI, sucrase-isomaltase; NHE3, sodium-hydrogen exchanger 3. (D) SI on the apical surface sections of mock and RV-infected HIEs on a transwell. (Scale bar, 10 μm .) Magenta, SI; green, RV; blue, DAPI. (E) Parental and DGAT1^{-/-} (KO) whole mount HIEs were probed with antibodies to detect the indicated cellular proteins [red, SI; green, NHE3; magenta, E-cadherin; blue (DAPI), nuclei]. Bar, 10 μm .

DGAT1 degradation in HIEs leads to a phenotype that is similar to that exhibited in intestinal biopsies from children who have genetic DGAT1 deficiency (10). We propose that a global decrease in cellular translation, due to increased phosphorylation of the initiation factor eIF2 α , detected in both RV infection and DGAT1^{-/-} HIEs, is responsible for the loss of nutrient and ion transporters and junctional proteins required for normal enterocyte homeostatic function.

Various intracellular pathogens, such as the bacteria *Mycobacterium tuberculosis* and *Chlamydia trachomatis*, the protozoan parasites *Trypanosoma cruzi* and *Toxoplasma gondii*, and viruses induce LD biogenesis, but the mechanisms for induction are unknown (38). Viruses from the *Flaviviridae* family, dengue virus, hepatitis C virus (HCV), West Nile virus, and Zika virus, interact with

LDs to usurp the host lipid metabolism for their own viral replication and pathogenesis (39). DGAT1 plays a critical role in HCV replication. DGAT1 forms a complex with the HCV nonstructural protein NS5A and the capsid core protein and coloads both proteins onto the same DGAT1-generated LD, which is critical for viral particle production and infectious virion release (40). Both HCV-mediated shuttling of DGAT1 out of the ER and RV-mediated loss of DGAT1, decrease ER-localized DGAT1. Our study suggests that DGAT1 is a regulator of LD biogenesis.

A primary function of DGAT1 is to synthesize TAGs. This reaction directly competes with phospholipid synthesis; DGAT1 and DGAT2 commit DAG to the synthesis of TAGs rather than the synthesis of phospholipids (41). DGAT1-overexpressing cells show a decrease in the intracellular levels of both DAG and

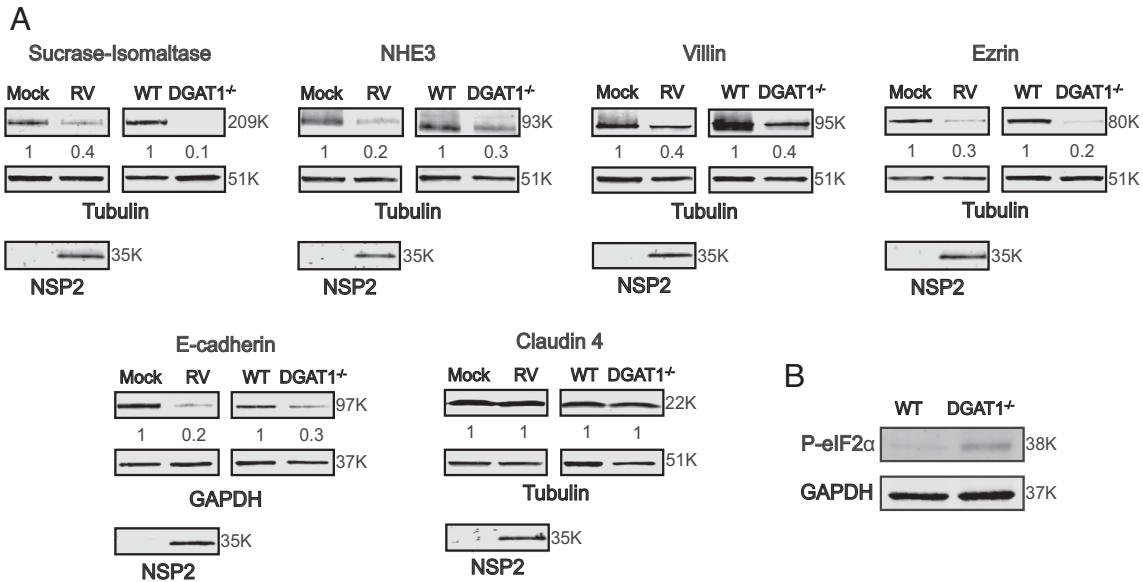


Fig. 4. RV-mediated DGAT1 degradation or DGAT1 deficiency in HIEs leads to loss of expression of apical brush border enzymes, cytoskeleton-binding proteins, and tight junctional proteins. (A) 3D HIEs were mock- or Ito-infected at a MOI of 10 and harvested at 24 hpi. Western blots of cell lysates prepared from mock- and RV-infected HIEs, and parental and DGAT1^{-/-} HIEs, were probed with antibody to detect the indicated proteins. Tubulin or GAPDH were detected as loading controls and NSP2 detected to indicate RV infection. The primary antibodies were detected with secondary antibodies conjugated to IRDye680RD and IRDye800CW. Infrared images of immunoblots were acquired using the Odyssey CLx and analyzed using Image Studio Lite software. Quantification of proteins normalized to tubulin or GAPDH with mock or WT set at 1 (n = 3) is shown below the respective blots. Molecular weights are indicated to the right of each blot. (B) Western blot of lysates from WT and DGAT1^{-/-} HIEs demonstrating a basal increase in P-eIF2 α in the DGAT1^{-/-} HIEs.

phospholipids, suggesting that phospholipid production and TAG synthesis share a pool of substrates (41). In the absence of DGAT1, where TAG synthesis is decreased, the pool of substrates can be diverted to phospholipid production. RV-mediated DGAT1 degradation may be the mechanism responsible for the increased synthesis of phospholipids (10, 32) that can then be used either for formation or growth of LDs or for membranes required for RV morphogenesis (12).

RV-mediated gastroenteritis is a multifactorial disease that includes malabsorption, which was previously thought to be due to destruction of the intestinal absorptive enterocytes. Malabsorption refers to decreased intestinal absorption of carbohydrate, protein, fat, minerals, or vitamins. We show that in RV-infected and DGAT1^{-/-} HIEs, the loss of expression of key proteins involved in nutrient absorption such as SI and villin substantiates reports that RV infection in children is associated with carbohydrate intolerance (42–45). SI aids in digestion of dietary carbohydrates such as starch, sucrose, and isomaltose. Villin, a calcium-regulated actin-binding protein, modulates the structure and assembly of actin filaments in microvilli responsible for nutrient uptake. We also found that expression of proteins involved in ion transport (NHE3) and cytoskeleton-binding (ezrin and E-cadherin) is drastically reduced. NHE3 is responsible for most water and sodium absorption in the intestine. Ezrin functions as a general cross-linker between plasma membrane proteins and the actin cytoskeleton that collaborate to build and maintain the apical domain and tight junctional integrity (46). The cell adhesion molecule E-cadherin is involved in transmitting chemical signals within cells and maintaining the normal structure of epithelial tissues. Cumulatively, decreased expression of these key proteins likely impair the structural integrity of the intestinal epithelium critical for proper gut function and absorption of fluid, solutes, and nutrients that can lead to malnutrition.

Symptoms associated with intestinal malabsorption include weight loss, diarrhea, greasy stools (due to high fat content), gas and abdominal bloating, and protein-losing enteropathy. RV infection has been associated with detection of fat in the stool of

infected children (47–49) and protein-losing enteropathy (50–54). While lack of expression of absorptive enzymes and apical ion transporters and functional changes in tight junctions between enterocytes that lead to paracellular leakage in RV-infected cells have been previously reported, the mechanisms that induce these changes were not defined (22, 55, 56). Our finding that DGAT1 degradation leads to the loss of expression of key nutrient and ion transporting proteins elucidates a pathophysiological mechanism of RV-mediated and DGAT1-deficiency malabsorptive diarrhea, with a possible mechanism of eIF2 α phosphorylation resulting in inhibition of global cellular translation.

A common mechanism for eIF2 α phosphorylation is the induction of the unfolded protein response (UPR), a homeostatic signaling network that orchestrates the recovery of ER stress (57). UPR involves signaling between the stress sensors protein kinase RNA-like ER kinase (PERK), inositol-requiring protein 1 α (IRE1 α), and activating transcription factor 6 (ATF6) (57). Activation of PERK initiates the phosphorylation of eIF2 α . RV infection activates two of the three arms of the UPR (IRE1 and ATF6), but not PERK (58, 59). However, eIF2 α is phosphorylated early during RV infection and remains phosphorylated throughout the replication cycle of the virus. RV-induced eIF2 α phosphorylation is dependent on the expression of three viral proteins, VP2, NSP2, and NSP5; silencing the expression of any of these three proteins inhibits eIF2 α phosphorylation and VI formation (34). Interestingly, eIF2 α phosphorylation is not required for RV replication since mutant cells that produce a nonphosphorylatable eIF2 α support virus replication as efficiently as wild-type cells (34). Our current data show that phosphorylation of eIF2 α may be involved in reduced brush border enzyme expression. Brush border enzymes may not be the only proteins with decreased expression as P-eIF2 α shuts down global cellular translation. However, lack of the brush border proteins appears to be responsible for the malabsorptive diarrhea observed in both RV-infected and DGAT1-deficient children. Future studies will determine whether RV infection-mediated DGAT1 degradation and DGAT1

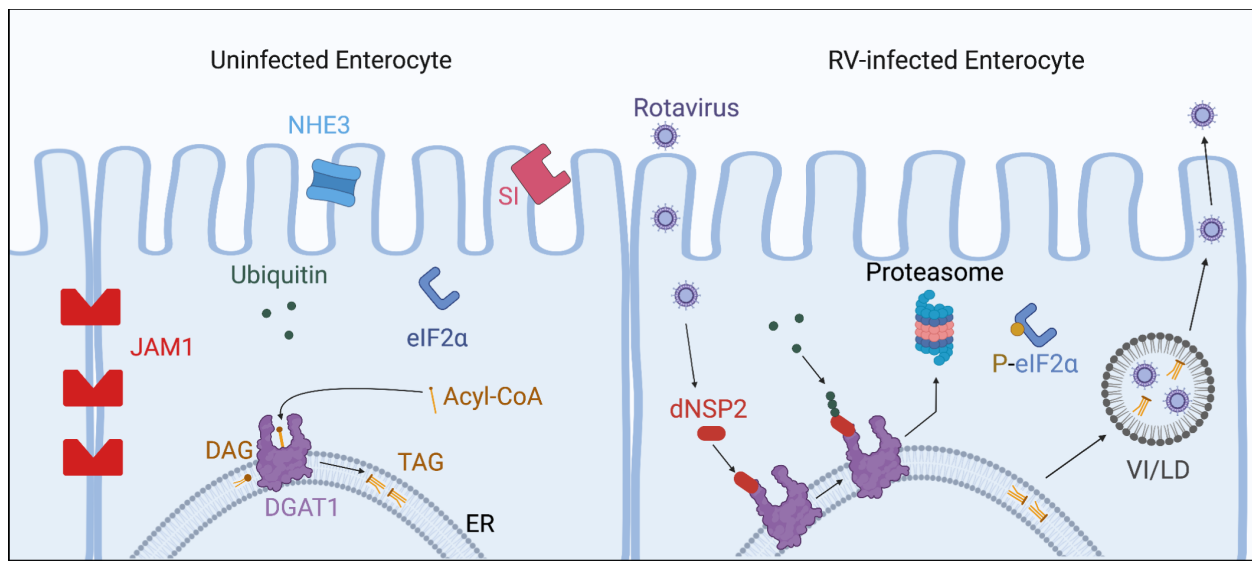


Fig. 5. Model of TAG and RV-induced LD biogenesis. (Left cell) The cartoon depicts the apical (luminal) side of an uninfected small intestinal enterocyte. Several homeostatic cellular functions are depicted. DGAT1, an ER transmembrane protein, synthesizes TAGs from ER-resident DAGs and cytoplasmic acyl-CoA. After synthesis by DGAT1, TAGs are deposited and accumulate in the ER lipid bilayer where it resides until needed. Under normal conditions, vital intestinal proteins are expressed and trafficked within the cell: JAM-1 to the tight junctions, and the sodium hydrogen antiporter 3 (NHE3) and sucrose-isomaltase (SI) to the apical surface. Eukaryotic initiation factor subunit 2 alpha (eIF2 α) associates with mRNA and ribosomal subunits for global protein translation. Cytoplasmic ubiquitin attaches to proteins for degradation in the proteasome. (Right cell) Proposed model of RV-mediated DGAT1 degradation, LD biogenesis, and inhibition of cellular protein synthesis. RV infects small intestinal epithelial cells and directs the expression of dNSP2. Cytoplasmic dNSP2 interacts with DGAT1 and is tagged with ubiquitin. The ubiquitin-tagged dNSP2/DGAT1 complex is degraded by the proteasome. RV-mediated loss of DGAT1 induces the budding of DGAT1-synthesized TAGs into LDs from the ER membrane. These LDs form into viroplasm/LD (VI/LD) complexes, the critical sites for initial virus replication. RV infection mediates eIF2 α phosphorylation, decreasing global cellular translation, including translation of NHE3 and SI, as well as the mislocalization of JAM-1. The loss or mislocalization of those proteins contributes to malabsorptive diarrhea induced by RV infection.

deficiency are responsible for the observed eIF2 α phosphorylation, the mechanism of eIF2 α phosphorylation as well as whether expression of other cellular proteins are affected.

While it is possible that RV infection mediates the degradation of other ER-localized proteins, we propose that RV-mediated DGAT1 degradation is responsible for the increase in viroplasm formation, RV yield, and eIF2 α phosphorylation. We demonstrated that dNSP2 interacts with another ER-localized lipid-modifying enzyme MGAT3 and the ER calcium release channel IP3R3. Even though dNSP2 interacts with each of these ER-localized proteins, DGAT1 does not interact with either MGAT3 or IP3R3 in RV-infected cells. In addition to DGAT1, DGAT2 also catalyzes DAG and acyl-CoA into TAG. Considering that RV only infects the mature (differentiated) epithelial cells of the human intestinal tract that do not express DGAT2, our results indicate that DGAT2 does not appear to play a role in RV replication or the reduction of expression of the tested cellular proteins. We show that 1) RV yield is increased in DGAT1 KO MEFs and overexpression of DGAT1 reduces virus yield; 2) differentiated HIEs only express DGAT1, but not DGAT2; 3) RV infection of differentiated HIEs does not induce DGAT2 expression; and 4) biopsies from DGAT1-deficient children and our differentiated DGAT1 KO HIE line indicate that loss of DGAT1 results in reduced expression or localization of the tested cellular proteins. Future studies will determine whether RV-mediated DGAT1 degradation alone or interaction with other ER-localized proteins is responsible for the increase in viroplasm formation, RV yield, and eIF2 α phosphorylation.

Based on our results, we propose a model of RV-induced viroplasm/LD (VI/LD) complex formation (Fig. 5). In uninfected enterocytes (Fig. 5, *Left*), ER-localized DGAT1 synthesizes TAG from DAG and acyl-CoA and stores the TAG in the ER lipid bilayer. Following RV entry (Fig. 5, *Right*, not all steps in the RV replication cycle are shown in the figure) and particle uncoating, dsRNA

transcription and translation occur in the cytoplasm of the infected enterocyte. NSP2 is synthesized and expressed initially as dNSP2, dispersed throughout the cytoplasm. A subset of dNSP2 interacts with endogenous DGAT1, embedded in the ER membrane, and mediates the degradation of DGAT1 by the cellular proteasome. The degradation of DGAT1 1) induces LD formation, 2) attenuates global cellular translation through phosphorylation of eIF2 α , and 3) likely contributes to viral cellular lipid homeostasis alteration. The induced LDs associate with NSP2 and NSP5 and become VIs. The dsRNA genome is replicated inside the VI and immature viral particles are assembled. Once assembled, the DLP participates in a second wave of transcriptional expression of viral mRNA. Eventually, DLPs bud through viroplasm-adjacent COPII vesicle-derived membranes where they become fully mature triple layer particles. Meanwhile, as immature particles assemble, global protein translation remains shut down. Digestive proteins as well as cellular structure proteins are not expressed. Therefore, infected villi become stunted and unable to digest and absorb luminal contents. Intestinal contents remain unabsorbed, contributing to malabsorptive diarrhea. Our model suggests that DGAT1 degradation increases RV replication through induction of LD formation while also contributing to RV diarrhea.

Materials and Methods

Details of culturing African green monkey kidney cells (MA104), immortalized DGAT1^{-/-} and DGAT1^{+/+} mouse embryonic fibroblasts [(MEFs) kindly provided by Robert V. Farese Jr. (Harvard University, Boston, MA)] (60), HIEs, Simian RV strain SA11 4F [G3P6(1)], and human RV strain Ito [G3P8] are included in [SI Appendix](#).

Detailed methods and descriptions of antibodies and reagents; IP and western blots; immunofluorescence; HIE DGAT1 knockout transduction and single-cell cloning; metabolic labeling with BODIPY™ 558/568 C12; sodium dodecyl-sulfate polyacrylamide gel electrophoresis (SDS-PAGE) and western blot analysis; HIE

RNA-seq; and statistical analysis are provided in *SI Appendix, SI Materials and Methods*.

Data, Materials, and Software Availability. The sequencing data has been deposited in the National Center for Biotechnology Gene Expression Omnibus, <https://www.ncbi.nlm.nih.gov/geo/> (accession nos. GSE168005 (61) and GSE183222 (62)). All other data are included in the article and/or *SI Appendix*.

ACKNOWLEDGMENTS. This work was supported by NIH Grants R01 AI080656 and U19 AI116497 (to M.K.E. and S.E.C.) and 1S10OD028480. This project was also supported by the Advanced Technology Core Laboratories (Baylor College of Medicine),

specifically the Integrated Microscopy Core, the Mass Spectrometry Proteomics Core, and the Protein and Monoclonal Antibody Production Core with funding from P30 Cancer Center Support Grant (NCI-CA125123), P30 Digestive Disease Center (NIDDK-56338-13/15), CPRIT (RP150578), and the John S. Dunn Gulf Coast Consortium for Chemical Genomics. Portions of this paper were previously included as part of Zheng Liu's dissertation.

Author affiliations: ^aDepartment of Molecular Virology and Microbiology, Baylor College of Medicine, Houston, TX 77030; ^bDepartment of Biosciences, Rice University, Houston, TX 77005; and ^cDepartment of Medicine, Baylor College of Medicine, Houston, TX 77030

1. J. A. Olzmann, P. Carvalho, Dynamics and functions of lipid droplets. *Nat. Rev. Mol. Cell Biol.* **20**, 137–155 (2019).
2. K. Tauchi-Sato, S. Ozeki, T. Houjou, R. Taguchi, T. Fujimoto, The surface of lipid droplets is a phospholipid monolayer with a unique fatty acid composition. *J. Biol. Chem.* **277**, 44507–44512 (2002).
3. A. R. Thiam, L. Foret, The physics of lipid droplet nucleation, growth and budding. *Biochim. Biophys. Acta* **1861**, 715–722 (2016).
4. J. Chung *et al.*, LDAF1 and seipin form a lipid droplet assembly complex. *Dev. Cell* **51**, 551–563.e7 (2019).
5. A. Pol, S. P. Gross, R. G. Parton, Review: Biogenesis of the multifunctional lipid droplet: Lipids, proteins, and sites. *J. Cell Biol.* **204**, 635–646 (2014).
6. S. Cases *et al.*, Cloning of DGAT2, a second mammalian diacylglycerol acyltransferase, and related family members. *J. Biol. Chem.* **276**, 38870–38876 (2001).
7. S. J. Stone *et al.*, The endoplasmic reticulum enzyme DGAT2 is found in mitochondria-associated membranes and has a mitochondrial targeting signal that promotes its association with mitochondria. *J. Biol. Chem.* **284**, 5352–5361 (2009).
8. J. T. Haas *et al.*, DGAT1 mutation is linked to a congenital diarrheal disorder. *J. Clin. Invest.* **122**, 4680–4684 (2012).
9. J. M. van Rijn *et al.*, Intestinal failure and aberrant lipid metabolism in patients with DGAT1 deficiency. *Gastroenterology* **155**, 130–143.e15 (2018).
10. C. Schlegel *et al.*, Reversible deficits in apical transporter trafficking associated with deficiency in diacylglycerol acyltransferase. *Traffic* **19**, 879–892 (2018).
11. P. Roingeard, R. C. Melo, Lipid droplet hijacking by intracellular pathogens. *Cell Microbiol.* **19**, e12688 (2017).
12. S. E. Crawford *et al.*, Rotavirus infection. *Nat. Rev. Dis. Primers* **3**, 17083 (2017).
13. W. Cheung *et al.*, Rotaviruses associate with cellular lipid droplet components to replicate in viroplasm, and compounds disrupting or blocking lipid droplets inhibit viroplasm formation and viral replication. *J. Virol.* **84**, 6782–6798 (2010).
14. I. Afrikanova, E. Fabbretti, M. C. Miozzo, O. R. Burrone, Rotavirus NSP5 phosphorylation is up-regulated by interaction with NSP2. *J. Gen. Virol.* **79**, 2679–2686 (1998).
15. T. Lopez, M. Rojas, C. Ayala-Breton, S. Lopez, C. F. Arias, Reduced expression of the rotavirus NSP5 gene has a pleiotropic effect on virus replication. *J. Gen. Virol.* **86**, 1609–1617 (2005).
16. Y. Kim *et al.*, Novel triacsin C analogs as potential antivirals against rotavirus infections. *Eur. J. Med. Chem.* **50**, 311–318 (2012).
17. J. M. Criglar *et al.*, Phosphorylation cascade regulates the formation and maturation of rotaviral replication factories. *Proc. Natl. Acad. Sci. U.S.A.* **115**, E12015–E12023 (2018).
18. C. Bomidi, M. Robertson, C. Coarfa, M. K. Estes, S. E. Blatt, Single-cell sequencing of rotavirus-infected intestinal epithelium reveals cell-type specific epithelial repair and tuft cell infection. *Proc. Natl. Acad. Sci. U.S.A.* **118**, e2112814118 (2021).
19. N. C. Zachos *et al.*, Human rotavirus diarrhea is associated with altered trafficking and expression of apical membrane transport proteins. *bioRxiv* [Preprint] (2019). <https://doi.org/10.1101/784264> (Accessed 20 October 2020).
20. J. A. Boshuizen *et al.*, Changes in small intestinal homeostasis, morphology, and gene expression during rotavirus infection of infant mice. *J. Virol.* **77**, 13005–13016 (2003).
21. G. Obert, I. Peiffer, A. L. Servin, Rotavirus-induced structural and functional alterations in tight junctions of polarized intestinal Caco-2 cell monolayers. *J. Virol.* **74**, 4645–4651 (2000).
22. K. G. Dickman *et al.*, Rotavirus alters paracellular permeability and energy metabolism in Caco-2 cells. *Am. J. Physiol. Gastrointest. Liver Physiol.* **279**, G757–G766 (2000).
23. K. Saxena *et al.*, Human intestinal enteroids: A new model to study human rotavirus infection, host restriction, and pathophysiology. *J. Virol.* **90**, 43–56 (2016).
24. K. Saxena *et al.*, A paradox of transcriptional and functional innate interferon responses of human intestinal enteroids to enteric virus infection. *Proc. Natl. Acad. Sci. U.S.A.* **114**, E570–E579 (2017).
25. J. M. Criglar *et al.*, A genetically engineered rotavirus NSP2 phosphorylation mutant impaired in viroplasm formation and replication shows an early interaction between vNSP2 and cellular lipid droplets. *J. Virol.* **94**, e00972–20 (2020).
26. J. M. Criglar *et al.*, A novel form of rotavirus NSP2 and phosphorylation-dependent NSP2-NSP5 interactions are associated with viroplasm assembly. *J. Virol.* **88**, 786–798 (2014).
27. J. L. Martinez, C. Eichwald, E. M. Schraner, S. Lopez, C. F. Arias, Lipid metabolism is involved in the association of rotavirus viroplasm with endoplasmic reticulum membranes. *Virology* **569**, 29–36 (2022).
28. E. R. Gaunt, W. Cheung, J. E. Richards, A. Lever, U. Desselberger, Inhibition of rotavirus replication by downregulation of fatty acid synthesis. *J. Gen. Virol.* **94**, 1310–1317 (2013).
29. G. L. Grice, J. A. Nathan, The recognition of ubiquitinated proteins by the proteasome. *Cell Mol. Life Sci.* **73**, 3497–3506 (2016).
30. J. M. van Rijn *et al.*, DGAT2 partially compensates for lipid-induced ER stress in human DGAT1-deficient intestinal stem cells. *J. Lipid. Res.* **60**, 1787–1800 (2019).
31. I. H. Holmes, B. J. Ruck, R. F. Bishop, G. P. Davidson, Infantile enteritis viruses: Morphogenesis and morphology. *J. Virol.* **16**, 937–943 (1975).
32. E. R. Gaunt *et al.*, Lipidome analysis of rotavirus-infected cells confirms the close interaction of lipid droplets with viroplasm. *J. Gen. Virol.* **94**, 1576–1586 (2013).
33. H. P. Harding *et al.*, Regulated translation initiation controls stress-induced gene expression in mammalian cells. *Mol. Cell* **6**, 1099–1108 (2000).
34. H. Montero, M. Rojas, C. F. Arias, S. Lopez, Rotavirus infection induces the phosphorylation of eIF2alpha but prevents the formation of stress granules. *J. Virol.* **82**, 1496–1504 (2008).
35. M. Rojas, C. F. Arias, S. Lopez, Protein kinase R is responsible for the phosphorylation of eIF2alpha in rotavirus infection. *J. Virol.* **84**, 10457–10466 (2010).
36. T. C. Walther, R. V. Farese Jr., Lipid droplets and cellular lipid metabolism. *Annu. Rev. Biochem.* **81**, 687–714 (2012).
37. M. Bosch, M. J. Sweet, R. G. Parton, A. Pol, Lipid droplets and the host-pathogen dynamic: FAF4 attraction? *J. Cell Biol.* **220**, e202104005 (2021).
38. E. Herker, M. Ott, Emerging role of lipid droplets in host/pathogen interactions. *J. Biol. Chem.* **287**, 2280–2287 (2012).
39. J. Zhang, Y. Lan, S. Sanyal, Modulation of lipid droplet metabolism—A potential target for therapeutic intervention in flaviviridae infections. *Front. Microbiol.* **8**, 2286 (2017).
40. G. Camus *et al.*, Diacylglycerol acyltransferase-1 localizes hepatitis C virus NS5A protein to lipid droplets and enhances NS5A interaction with the viral capsid core. *J. Biol. Chem.* **288**, 9915–9923 (2013).
41. C. Bagnato, R. A. Igal, Overexpression of diacylglycerol acyltransferase-1 reduces phospholipid synthesis, proliferation, and invasiveness in simian virus 40-transformed human lung fibroblasts. *J. Biol. Chem.* **278**, 52203–52211 (2003).
42. J. Q. Trounce, J. A. Walker-Smith, Sugar intolerance complicating acute gastroenteritis. *Arch. Dis. Child.* **60**, 986–990 (1985).
43. R. M. Beattie, M. C. Vieira, A. D. Phillips, N. Meadows, J. A. Walker-Smith, Carbohydrate intolerance after rotavirus gastroenteritis: A rare problem in the 1990s. *Arch. Dis. Child.* **72**, 466 (1995).
44. S. Ostakul, S. Arunchiya, A. Puetpaiboon, L. Lebel, Incidence and risk factors for carbohydrate intolerance in Thai infants with acute diarrhoea: An outpatient-based study. *Southeast Asian J. Trop. Med. Public Health* **27**, 780–784 (1996).
45. H. Szajewska, M. Kantecki, P. Albrecht, J. Antoniewicz, Carbohydrate intolerance after acute gastroenteritis—a disappearing problem in Polish children. *Acta Paediatr.* **86**, 347–350 (1997).
46. J. B. Casaleto, I. Saotome, M. Curto, A. I. McClatchey, Ezrin-mediated apical integrity is required for intestinal homeostasis. *Proc. Natl. Acad. Sci. U.S.A.* **108**, 11924–11929 (2011).
47. F. Chowdhury, A. I. Khan, M. I. Hossain, M. A. Malek, A. S. Faruque, Presence of neutral fat in stool and its association with aetiology and presenting features of diarrhoea in children. *Trop. Gastroenterol.* **26**, 80–84 (2005).
48. A. S. Mizanur Rahman, Neutral fat in stool as clinical indicator of rotavirus diarrhoea in under-five children. *J. Trop. Pediatr.* **36**, 265–266 (1990).
49. M. E. Thomas, P. Luton, J. Y. Mortimer, Virus diarrhoea associated with pale fatty faeces. *J. Hyg. (Lond.)* **87**, 313–319 (1981).
50. T. Iwasa, N. Matsubayashi, Protein-losing enteropathy associated with rotavirus infection in an infant. *World J. Gastroenterol.* **14**, 1630–1632 (2008).
51. S. S. Bharwani, Q. Shaukat, R. Basak, A 10-month-old with rotavirus gastroenteritis, seizures, anasarca and systemic inflammatory response syndrome and complete recovery. *BMJ Case Rep.* **2011**, bcr0420114126 (2011).
52. B. Aldemir-Kocabas, A. Karbuz, E. Ciftci, M. Demir, E. Ince, An unusual cause of secondary capillary leak syndrome in a child: Rotavirus diarrhea. *Turk. J. Pediatr.* **55**, 90–93 (2013).
53. M. Trivedi, A. Jain, D. Shah, P. Gupta, Rotavirus gastroenteritis associated with encephalopathy, myositis, transaminitis and hyposalbuminemia. *Indian J. Pediatr.* **86**, 642–644 (2019).
54. A. Parisi *et al.*, Protein-losing enteropathy in an infant with rotavirus infection. *Paediatr. Int. Child Health* **38**, 154–157 (2018).
55. I. Beau, A. Berger, A. L. Servin, Rotavirus impairs the biosynthesis of brush-border-associated dipeptidyl peptidase IV in human enterocyte-like Caco-2/TC7 cells. *Cell Microbiol.* **9**, 779–789 (2007).
56. S. Martin-Latil *et al.*, A cyclic AMP protein kinase A-dependent mechanism by which rotavirus impairs the expression and enzyme activity of brush border-associated sucrase-isomaltase in differentiated intestinal Caco-2 cells. *Cell Microbiol.* **6**, 719–731 (2004).
57. C. Hetz, The unfolded protein response: Controlling cell fate decisions under ER stress and beyond. *Nat. Rev. Mol. Cell Biol.* **13**, 89–102 (2012).
58. V. Trujillo-Alonso, L. Maruri-Avidal, C. F. Arias, S. Lopez, Rotavirus infection induces the unfolded protein response of the cell and controls it through the nonstructural protein NSP3. *J. Virol.* **85**, 12594–12604 (2011).
59. S. Lopez, A. Ocegüera, C. Sandoval-Jaime, Stress response and translation control in rotavirus infection. *Viruses* **8**, 162 (2016).
60. C. A. Harris *et al.*, DGAT enzymes are required for triacylglycerol synthesis and lipid droplets in adipocytes. *J. Lipid. Res.* **52**, 657–667 (2011).
61. S. E. Blatt *et al.*, Data from "Use of human tissue stem cell-derived organoid cultures to model enterohepatic circulation." Gene Expression Omnibus. <https://www.ncbi.nlm.nih.gov/brum.beds.ac.uk/geo/query/acc.cgi>. Accessed 25 March 2022.
62. S. E. Crawford, S. E. Blatt, Z. K. Criss, M. K. Estes, N. F. Shroyer, Data from "Drivers of transcriptional variance in human intestinal epithelial organoids." Gene Expression Omnibus. <https://www.ncbi.nlm.nih.gov/brum.beds.ac.uk/geo/query/acc.cgi>. Accessed 25 March 2022.